Published in final edited form as:
J Phys Chem B. 2013 September 5; 117(35): . doi:10.1021/jp401512z.

Simulations of Anionic Lipid Membranes: Development of Interaction-Specific Ion Parameters and Validation using NMR Data

Richard M. Venable[1], **Yun Luo**[2,§], **Klaus Gawrisch**[3], **Benoît Roux**[4], and **Richard W. Pastor**[1,*]

[1]Laboratory of Computational Biology, National Heart, Lung, and Blood Institute, National Institutes of Health, Bethesda, MD 20892

[2]Argonne Leadership Computing Facility, Argonne National Laboratory, Argonne, IL 60439

[3]Laboratory of Membrane Biochemistry & Biophysics, National Institute on Alcohol Abuse and Alcoholism, National Institutes of Health, Bethesda, MD 20892

[4]Department of Biochemistry and Molecular Biology, The University of Chicago, Chicago, IL 60637

Abstract

Overbinding of ions to lipid head groups is a potentially serious artifact in simulations of charged lipid bilayers. In this study, the Lennard-Jones radii in the CHARMM force field for interactions of Na^+ and lipid oxygen atoms of carboxyl, phosphate and ester groups were revised to match osmotic pressure data on sodium acetate, and electrophoresis data on palmitoyloleoyl phosphatidylcholine (POPC) vesicles. The new parameters were then validated by successfully reproducing previously published experimental NMR deuterium order parameters for dimyristoyl phosphatidylglycerol (DMPG) and newly obtained values for palmitoyloleoyl phosphatidylserine (POPS). Although the increases in Lennard-Jones diameters are only 0.02 to 0.12 Å, they are sufficient to reduce Na+ binding, and thereby increase surface areas per lipid by 5–10% compared with the unmodified parameters.

Introduction

Additive force fields (FF) for biological molecules that form a variety of complex phases have seen continuing development, especially the widely used CHARMM[1] force fields, which are supported by many biomolecular simulation software packages besides CHARMM itself, including AMBER,[2] DESMOND[3] (and ANTON), GROMACS,[4] LAMMPS,[5] and NAMD.[6] The recent C36 update of the CHARMM lipid FF[7] resolved a number of issues,[8] notably the ability to use the tensionless NPT ensemble for neutral zwitterionic lipids such as those with phosphatidylcholine (PC) and phosphatidylethanolamine (PE) head groups. Validation for PC and PE lipid types was straightforward, due to the abundance of complementary experimental target data available. The extension of the FF to charged lipids requires further consideration of ion/lipid interaction given the importance of ion binding to the charged membranes. The presence of strong binding of Na+ to lipid head group atoms in simulations, and the lack of consensus among these studies has been a long-standing concern in the field.[9,10]

*Corresponding author: pastorr@nhlbi.nih.gov.
§Present address: Western University of Health Sciences, College of Pharmacy, Pharmaceutical Sciences Department, 309 E. Second St., Pomona, CA 91766-1854

The focus of the present work is the interaction of Na^+ and lipid oxygen atoms of carboxyl, phosphate and ester groups. It is based on the approach introduced by Roux and coworkers[11,12] in which the Lennard-Jones (LJ) well depth E_{min} and diameter R_{min} for cations and selected heterogeneous interactions is not calculated from the standard arithmetic combining rule, but, rather, is parametrized separately for the selected atom pair. Values for R_{min} for selected oxygens were determined in one of two ways for the present study. Over-binding of sodium and carboxylate moiety was assessed by monitoring the amount of ion pairing in a concentrated sodium-acetate solution and its impact on the resulting osmotic pressure is deduced using the simulation method of Yun and Roux.[13] Optimized pair-specific parameters were then obtained by matching the measured osmotic pressure as a function of concentration. The sodium interactions with phosphate and ester carboxylate are refined by minimizing the effective charge of palmitoyloleoyl phosphatidylcholine (POPC) bilayers. The rational for this strategy is elaborated in the following paragraph. The procedure for minimizing the charges utilized the newly developed "Harmonic Restraint Method" is presented in the Methods.

Electrophoresis measurements might be expected to yield valuable target data for parameterization of charged lipids. Specifically, the experimentally measured electrophoretic mobility μ is converted into the ζ-potential using the Helmholtz-Smoluchowski equation:

$$\zeta = \mu\eta/(\varepsilon_a\varepsilon_0) \quad (1)$$

where η and is the viscosity of the aqueous solution with dielectric constant ε_w, and ε_0 is the vacuum permittivity. The ζ-potential is then defined as the electrostatic potential at the plane of zero-shear near the membrane surface.[14,15] However, a consistent and general theoretical framework for relating the concepts of membrane electrophoretic mobility and ζ-potential with the average Galvani phase potential obtained from MD simulations based on all-atom models remains to be developed. Additionally, estimates of electrostatic Galvani phase potentials from simulation are extremely sensitive to placement of charges on the molecule.[16–18] Nevertheless, one experimental observation is straightforward to use: bilayer vesicles containing only neutral lipids such as POPC do not migrate in an electric field at any sodium chloride concentration.[19] Hence, by Eq (1), ζ=0 (to within the experimental accuracy of approximately ±3 mV). This is not a trivial or obvious result. For example, a fraction of Na^+ could directly bind to the negatively charged phosphate group while Cl^- essentially behaves as an atmosphere of solvated mobile counterions in the bulk solution, leaving a vesicle with a net positive charge and the propensity to migrate in an applied field. Hence, valid sodium-lipid interaction force field parameters should, as a prerequisite, minimize the over-binding of sodium with the negatively charged phosphate moiety and yield a correct response of a POPC bilayer to an applied electric field. The results are compared with Gouy-Chapman theory[14] in the Discussion.

The revised parameters are validated by comparing NMR deuterium order parameters, $|S_{CD}|$, from simulations of lipid bilayers with those of experiment. As demonstrated in previous studies,[20–22] chain order parameters are a practical surrogate for the surface area per lipid, A_ℓ, a now-standard target for parameterization because it is both biologically important and highly sensitive to imbalances in the FF.[23] Values of A_ℓ can be inferred from x-ray and neutron diffraction experiments, and are available for a number of neutral lipids though relatively few charged ones. A x-ray study by Petrache et al.[24] on dioleoyl phosphatidylserine (DOPS) in the absence of added salt indicated an area/lipid of 65.3 $Å^2$ for the fluid phase at 30 °C. Corresponding experiments for POPS, which more closely resembles biological PS lipids with its saturated sn-1 chain, were not available, although an MD simulation study[25] suggested an area/lipid of about 55 $Å^2$ for this lipid. An area/lipid of

ca. 62 Å^2 was inferred for dimyristoyl phosphatidylglycerol (DMPG) from older Langmuir trough experiments,[26] though assumptions are required to relate the area on a monolayer isotherm to that of an bilayer at equilibrium. In contrast, the lipid chain NMR deuterium order parameters, $|S_{CD}|$, are relatively easy to obtain for charged lipids. Simulations of saturated neutral lipids yield values of both A_ℓ and $|S_{CD}|$ that are in very good agreement with experiment,[7] and it is therefore reasonable to propose that agreement of simulated and experimental order parameters for other fluid phase bilayers can be regarded to be a good measure of the accuracy of the simulation. A detailed study of DMPG phase behavior published in 2011 by Lowe, et al.[27] includes chain order parameter data as a function of $[Na^+]$ and temperature for a number of systems suitable for MD simulations. These order parameters and previously unreported measurements of bilayers with POPS are used for validation in the present study. PG and PS head groups are shown in Fig 1.

Methods

Simulation Programs

The CHARMM program[1] was used for all model building, and for the sodium parameter validation simulations and subsequent extraction of data for analyses; version c35b6 was used for the POPS simulations, while c36b2 was used for the DMPG simulations. NAMD[6] version 2.8 was used for the effective charge simulations, and for the osmotic pressure simulations.

Molecular Parameters

The recent CHARMM C36 lipid parameters[7] were used for the lipids in this study. The TIP3P water model[28] as modified[29] for CHARMM was used as the solvent. Three different Na^+ ion parameterized Lennard-Jones (LJ) models were employed. The first is the 1994 set of Beglov and Roux[30] denoted BR, which was included with the initial C36 lipid distribution. The second is the 2008 revised set of Noskov and Roux,[31] denoted NR, which includes non-bond pairwise exceptions for the Na^+ and Cl^- ion pair from Luo and Roux;[13] the CHARMM keyword for such exceptions is NBFIX, and can be applied to any specified pair. Finally, there is the current work, denoted CW, which corresponds to the NR set with additional NBFIX terms for Na^+ ions interacting with oxygen atoms occurring in carboxylate, carboxylate ester, and phosphate ester groups. CHARMM FF may be downloaded from http://mackerell.umaryland.edu/CHARMM_ff_params.html

Osmotic Pressure Simulations

The models at different concentrations were initially built by randomly replacing a number of water molecules by ions, within an equilibrated cubic box of TIP3P water molecules, with an edge length of 48 Å. The number of ions within the box was chosen according to the molar scale (i.e., concentrations were set from the number of ions per unit of volume of the simulated system). The equilibrium run contains a short minimization and a 400 ps equilibrium simulation at constant volume and temperature (300 K) with a Langevin thermostat and a damping coefficient of 0.05 ps^{-1}. It was followed by further equilibration under constant temperature and pressure (NPT) condition at 300 K and 1 atm using Langevin thermostat and a modified Nosé-Hoover method in which Langevin dynamics is used to control fluctuations in the barostat. Periodic boundary conditions were applied. The geometry of the TIP3 water molecules was constrained using the SHAKE algorithm. A multiple time-step integration scheme was used, with 1 fs for the calculation of the internal energy terms, and 2 fs for the calculation of the LJ and electrostatics terms. The electrostatic interactions were treated using PME. A smooth real space cutoff was applied between 10 and 12 Å with grid density of approximately 1 Å and a sixth-order interpolation of the charge to the grid. The same cutoff was used for the LJ potential with a switching function.

After equilibration to a converged volume, the production run is carried out using NVT ensemble. Following the virtual membrane method used previously for sodium chloride,[13] comparable osmotic pressure simulations were performed for both sodium acetate and sodium dimethylphosphate. The z length was expanded to ca. 91 Å by appending an extra water box, with the virtual membrane placed to separate the bulk region and salt solution region. The virtual membrane is a harmonic restraint acting only on the ions, representing the effect of an ideal semipermeable membrane. The molar concentrations employed were 0.5, 1.0, 2.0, and 3.0 for acetate, and 0.5, 0.75, 1.0, 1.5, and 2.0 for dimethylphosphate. Ten replicates of 2 ns each were generated. For sodium acetate, the procedure was iterated with alternate $R^{ij}_{\min}$ values for the Na^+:O^- pairs in order to optimize this parameter.

Harmonic Restraint Method and Simulations

This new method was developed to determine the effective charge Q_{eff} of a lipid bilayer by simulating its response to an applied electric field E. Specifically, the bilayer (or any large or small molecular assembly) is constrained in a harmonic potential with force constant k, and the average displacement $\overline{\Delta d}$ along the direction of the field is evaluated. The force on the bilayer from the field is Q_{eff}E. This is balanced by the force from the constraint, $k\overline{\Delta d}$, leading to

$$Q_{eff}=k\overline{\Delta d}/E \quad (2)$$

Q_{eff} can be evaluated from simulations with a single field or from the slope of $\overline{\Delta d}$ vs. E.

For purposes of parameter development, the effective charge method complements the osmotic pressure method: (1) it can be applied directly to bilayers; (2) it can be applied to interactions with uncharged functional groups, such as carboxylate esters. The osmotic pressure approach, in contrast, is applicable to small molecules. While it can be applied to uncharged species, the osmotic pressure dependence on ionic concentration is too small to be a useful target for the present parameter development.

An existing 72 POPC lipid bilayer[7] with ca. 31 waters/lipid was expanded along z by adding water to reach 120 waters/lipid. To obtain a 0.1 M NaCl solution, 16 Na^+ and 16 Cl^- ions were added via random water replacement, as described below for the POPS bilayer. The simulation method is the same as for osmotic pressure calculation. After equilibration to a converged volume, four simulations were run in the NVT ensemble, each with an external electric field E = 0.4 kcal/mol $Å^{-1}e^{-1}$ applied in one of the x, −x, y, or −y directions, with a harmonic restraint k= 1.0 kcal/mol $Å^{-2}$ applied on the bilayer center of mass. As noted in the Introduction, the strategy here is based on the results of electrophoresis experiments, where vesicles of POPC do not migrate in an applied electric field, indicating that their net charge is very close to zero. The $R^{ij}_{\min}$ values for sodium paired with O atoms in ester C=O and P=O functional groups were therefore adjusted iteratively to minimize the effective charge.

Validation of the Harmonic Restraint Method

This subsection provides further validation for the harmonic restraint method using sodium acetate. Three methods for calculating the effective charge Q_{eff} are compared for the acetate ion in NaCl aq. solution. Model building and simulation techniques were identical to those described for the osmotic pressure simulations in the Methods section. System sizes (number of ions and water molecules) are listed in Table 1.

Drift velocity—An external electric field was applied in the *z* direction with different magnitudes. The electric field determines the average drift velocities of ions and the distances traveled by them. Constant drift velocities were observed in our simulations. The magnitudes of electric field were chosen from 0.2 to 1.8 kcal $mol^{-1}Å^{-1}e^{-1}$. The drift velocity *v* determines the ionic mobility μ at constant electric field: $\mu=\langle v\rangle/E$. The mobility was obtained from a least squares fit of the drift velocity as a function of electric field magnitudes. Fig. 2 shows the drift velocity of acetate ion in different solutions. The electrophoretic mobilities ($Å^2\ ps^{-1}mV^{-1}$) of acetate ion in different NaCl aq. concentrations are included in Table 1. The effective charge is then

$$Q_{eff}=\mu\gamma \quad (3)$$

where γ is the drag coefficient and is a constant for our systems. The effective charge of acetate ion at 1 M NaCl aq. solution is approximated by the ratio of the mobility at this concentration to the mobility of acetate in pure water solvent: $-\mu(c_1)/\mu(c_0) = -0.74$ e.

Einstein-Smoluchowski relation—The effective charge can also be calculated by

$$Q_{eff}=\mu k_B T/D_0 \quad (4)$$

where μ is still the mobility, k_BT is the Boltzmann constant times temperature and D_0 is the diffusion constant in the absence of an electric field,[32] which is calculated from the mean-square displacements (MSD) of the acetate ion in bulk solution 0.21 $Å^2$/ps. Using the mobility data from the previous drift velocity calculation, the effective charge of acetate ion at 1 M NaCl aq. solution is approximately −0.62 e.

Harmonic Restraint—Neither of the two preceding methods can presently be applied to a large assembly such as a lipid vesicle. This motivated the development of the harmonic restraint method already described above. For the present testing on the acetate, three different force constants were applied: k = 0.2, 0.5, 1.0 kcal $mol^{-1}Å^{-2}$. From the results shown in Fig. 3 and Eq (2), and the effective charge of acetate ion in 1 M NaCl aq. solution is −0.63 e.

The calculated effective charge of an acetate ion in 1 M NaCl aq. solution from 3 methods described above is summarized in Table 2. The consistency of those results indicates that the electrophoretic mobility and the effective charge calculated from those methods are reliable. The harmonic restraint method has the advantage of fast convergence, thus is used to calculate the effective charge of the lipid bilayer.

Parameter validation simulation conditions

The following conditions are common to all POPS and DMPG simulations used to validate the revised sodium parameters. Barostats and thermostats employed the extended system method for planar interfaces[33] for the NPT and NPAT ensembles. Electrostatics were evaluated using particle-mesh Ewald[34] with ca. 1 grid point per Å, a 6^{th}-order spline interpolation for the complementary error function, a κ value of 0.32, and a 12 Å real space cutoff. The van der Waals term used a standard 6–12 L-J form, with force switched truncation over the range of 10–12 Å. Explicit image periodic boundaries with a tetragonal prism unit cell (a=b by constraint) were employed, with heuristic updates of both non-bond and image atom lists. The SHAKE constraint method was applied to all covalent bonds to hydrogen, with the default 1.0×10^{-10} Å tolerance. The integration time step was 1.0 fs, and coordinate sets were saved every ps.

POPS bilayer simulations

Seven initial aqueous bilayer models of 72 lipids (36 per leaflet) were constructed at an area/lipid of 70 $Å^2$, using the *de novo* procedure described previously.[7] After hydration to ca. 34–35 waters/lipid, the total charge of the system was adjusted to zero by random replacement of 72 water molecules with sodium ions, with a 5.5 Å exclusion region around the lipids and previously placed ion (random water replacement). Multiple ion placements were generated for each of the 7 bilayer models, and the lowest energy placement was chosen. Each model was subjected to 2 ns NPT equilibration simulations with a barostat piston mass of 1000 amu, heating from 203 K to 303 K over 100 ps, followed by 400 ps of thermal equilibration with the 3-step Verlet algorithm; the remaining 1.5 ns employed the Hoover thermostat. A consensus area/lipid of 64 $Å^2$ was obtained using data from the final ns of each simulation, and a coordinate set matching that area/lipid was selected from one of the models. The hydration was increased to 119 waters/lipid, giving a larger water layer; using random water replacement, 16 more Na^+ ions were added, along with 16 Cl^- ions, yielding a nominal 0.1 M excess of NaCl. The molarity for the bilayers was computed based on the H_2O/Na^+ ratio and the assumption that water is 55.5 M, i.e. one ion for every 555 water molecules. This system was equilibrated for 30 ns using the NPAT ensemble, and the final 20 ns were evaluated to determine the extent of bulk phase water, based on ion distributions and water dipole orientation along the bilayer normal (equated to the z-axis here).[35] Based on these criteria, a reduced hydration level of 58 waters/lipid was chosen for subsequent NPT simulations, with 8 NaCl pairs needed for the target 0.1 M excess salt. The final coordinate set from the 30 ns NPAT simulation was modified by discarding solvent and ions proximal to the +z and −z cell boundaries, and re-adjusting the ion counts. Three new NPT simulations were begun, with the ion treatments and trajectory lengths (the initial 10 ns of each was excluded from analysis) indicated in Table 3. Fig. 4 plots the area vs time for simulations of POPS for the assorted ion/lipid interaction parameters. Stable surface areas are attained by 10 ns for the CW set, justifying the 10 ns equilibration times. The ion binding lifetime data discussed later (Table 6) further supports this equilibration time. There is some further decrease in surface area at 40 ns for the NR set. However, the areas from NR and BR are in poor agreement with experiment (as judged by the lack of agreement with $|S_{CD}|$ to be described below), so the trajectories were terminated at 60 ns.

DMPG bilayer simulations

An initial model was constructed via the CHARMM-GUI web interface (http://www.charmm-gui.org), with a total of 72 lipids as for POPS, at a hydration level of 75 waters/lipid, and with 72 Na^+ ions for electrical neutrality. Additional DMPG bilayer models with 0.1 M excess NaCl were created by random water replacement, as described above for POPS. Four simulation systems were created, based on variations in the sodium parameters and excess NaCl concentration, as indicated in Table 3. Each was heated from 208 to 308 K over 100 ps, thermally equilibrated with the 3-step Verlet algorithm for an additional 900 ps, then continued under NPT conditions with the Hoover thermostat. Averages were accumulated after 10 ns, as supported by Fig. 5.

NMR of POPS bilayers

The lipid sample for NMR measurements was equilibrated in an excess of 0.1 M NaCl solution to eliminate uncertainties in ionic content due to the possible presence of minor amounts of salts in the dry lipid. About 10 mg of 1-perdeuterio-palmitoyl-2-oleoyl-*sn*-glycero-3-phosphoserine sodium salt (POPS-d_{31}; Avanti Polar Lipids, Inc., Alabaster, AL) were dispersed in 2 mL of 0.1 M NaCl solution prepared with deuterium-depleted water (Cambridge Isotope Laboratories, Inc., Andover, MA). The sample was homogenized by three freeze-thaw cycles, pelleted by ultracentrifugation and then transferred to a glass container sealed with a ground glass stopper. Before the NMR experiments, the sample was

kept frozen at −80 °C. NMR experiments were conducted on a DMX 500 spectrometer at a resonance frequency of 76.8 MHz using a solid-state 1H/X probe with a 5 mm solenoid coil (Bruker BioSpin, Billerica, MA). Spectra were acquired at a temperature of 30±0.5°C using a quadrupolar echo sequence, d_1-p/2-d_2-p/2^{90} –d_2-acqu, with delay times, d_1= 250 ms, d_2=50 ms, a pulse length p/2=2.7 ms, a spectral width of 200 kHz, 4 K data points, and 100,000 scans accumulated in quadrature detection mode. Spectra were processed and order parameters calculated with a program written for Mathcad (PTC, Needham, MA) as described previously.[36]

Results

Parameter revisions

As already noted, the sodium ion parameters of Noskov and Roux (NR)[31] based on the free energy of solvation, together with an NBFIX term developed via osmotic pressure simulations[13] for Na^+ with Cl^- served as the starting point, rather than the older Beglov and Roux LJ parameters (BR).[30] The well depth parameters, ε, were not modified. Table 4 provides the CHARMM nomenclature for relevant individual atoms, and their LJ radii.

In order to evaluate sodium ion interactions for NR with negatively charged lipid functional groups, osmotic pressure simulations were performed for sodium acetate and sodium dimethylphosphate over a range of concentrations. As evident in the top panel of Fig. 6, a large deviation from experiment is observed for the acetate anion. After iterative testing of adjustments to the $R^{ij}_{\min}$ value of the NBFIX term for the SOD:OCL pair, excellent agreement with experiment was obtained; the revised values are listed in Table 5.

The bottom panel in Fig. 6 indicates agreement with experiment for the NR parameters for dimethylphosphate, though the concentration range is lower than for acetate. Because the effective concentration of sodium can be higher near the bilayer surface (the location of the phosphates), simulations of a POPC bilayer were carried out in the presence of an electric field using harmonic restraints as described in the Methods. To test the method, simulations were first carried out at zero salt. No displacement was observed, ruling out artifacts resulting from concerted head group orientations or small system-size effects. In contrast, simulations at 0.1 M NaCl with the NR set led to statistically significant non-zero displacements corresponding to an effective charge per lipid of +0.032 e (Eq 2). As will be demonstrated in the following section, this value is out of the range consistent with the experimental observation, indicating over binding of Na^+ to the polar head groups. Potential binding sites include the oxygen atom on the phosphate group (O2L) and the carbonyl oxygen on the carboxylate ester group (OBL). The net charge was minimized to +0.0078 e/lipid by iteratively increasing $R^{ij}_{\min}$ for Na+ and the preceding two atom types to the values listed in Table 5.

NMR Spectroscopy

Fig. 7 shows the ^{2}H NMR spectrum of POPS-d_{31} at 30 °C. While carbons $C_{11–16}$ yield well-resolved quadrupolar splittings that are assigned directly, assignment of splittings to $C_{2–10}$ was done by integration, assuming a smooth decline of order parameters. The lower panel of Fig. 8 includes the experimental $|S_{CD}|$ ordered from largest to smallest. The precise assignment of splitting to carbon cannot be made because of signal overlap in the upper part of the chain. Hence the drop at carbon 3 evident in experiments of selectively deuterated chains[37] and simulation (Fig 8, top) is lost in the sorting. Nevertheless, a sufficiently clear plateau is evident, and this can be compared with simulations.

Validation simulations

Fig. 8 (top) plots $|S_{CD}|$ for the palmitate chain carbons from simulations of POPS using the three sets of sodium interaction parameters. BR and NR are comparable, and CW is noticeably lower, consistent with the larger area/lipid value (Table 3). The sorted values in Fig 8 (bottom) indicate that CW is in substantially better agreement with experiment.

Similar results are obtained for DMPG bilayers, again based on comparison to lipid chain order parameter determined via an NMR experiment. The top two panels of Fig. 9 show the simulation order parameters, grouped by lipid chain, and plotted as a function of chain position. As observed for POPS, CW noticeably lowers the order parameter profile, consistent with the larger area/lipid values reported in Table 3.

For both sets of sodium parameters, a small difference based on salt concentration is also observed. The lower 2 panels of Fig. 9 are grouped by concentration, and compare the simulation order parameters sorted by decreasing value to NMR values given for the average of the plateau region. In both cases, the horizontal line representing the NMR value crosses through an apparent plateau region, extending from sort indices 0 through 12; a clear drop is seen between 12 and 13.

Discussion and Conclusions

Molecular modeling and molecular dynamics simulations with additive (non-polarizable) force fields are now standard tools in structural biology, materials science, and related fields. It is in some sense remarkable that such force fields are so useful, given their relative simplicity of the representation of chemical structure, with atoms having fixed radii and fixed partial charges to describe non-bonded interactions. Not surprisingly, this leads to compromises in the development of force field parameters, as values that work well for matching one experimental observable may not work very well for matching some other measurement. It is also not surprising that extensions to the functional form, such as the combining rule for Lennard-Jones radii, are sometimes required.

The osmotic pressure results for sodium acetate in Fig. 6 (top) show quite clearly that LJ parameters for Na^+ based on the free energy of solvation in water[30,31] fail at sodium acetate concentrations above 1 M. While the concentration of ionic solutions in biological systems is typically within a range of 0.1–0.2 M, the local density of ions may far exceed this in the neighborhood of charged bilayer membranes formed with negatively charged lipids. Consequently, the observed deviation for sodium acetate is significant and indicates the need to use explicit non-bond exceptions (NBFIX terms), to adjust the interaction of Na^+ with carboxylate anions. An increase of only 0.12 Å to the LJ diameter for Na^+ and acetate oxygen (SOD-OCL in Table 5) is sufficient to yield an excellent match with experiment to 3 M. The corresponding concentration dependent study with dimethylphosphate anion agreed reasonably with experiment over a smaller concentration range (Fig 6, bottom). Most of the molecular mechanical force fields used currently in MD simulations have not been calibrated to guarantee that they will be accurate in all such situations. Tests with highly concentrated model systems must be conducted to verify the accuracy of the force field, and if needed, optimize the parameters or the functional forms.

There was also concern that sodium was over-binding to phosphate and carboxylate ester O atoms, atoms that are present in even neutral lipids. Simulations of POPC bilayers in 0.1 M NaCl using the newly developed Harmonic Restraint Method (described in the Methods) were then used to refine R^{ij}_{min} values for sodium ions with the O atoms double-bonded to P and C in phosphate and carboxylate esters, respectively. Unlike the osmotic pressure result, this method indicated an increase of 0.05 Å in R^{ij}_{min} for phosphate oxygen (SOD-O2L), and

0.02 Å for the ester oxygen (SOD-OBL) (Table 5). These refinements were based on the assumption that that the effective charge of a POPC vesicle is close to zero, as inferred from the lack of mobility (or zero ζ-potential) in an applied electric field.[19]

As already noted in the Introduction, the direct calculation of a ζ-potential from a simulation requires significant assumptions and is potentially unreliable. However, it is straightforward to estimate the ζ-potential from the Gouy-Chapman equation, which relates a uniform surface charge density σ and electric potential $\psi(0)$ at a flat surface, as follows:[14]

$$\sigma = \sqrt{c}\sqrt{8N\varepsilon_r\varepsilon_0 k_B T}\left(\frac{1}{2}\right)\left[exp\left(\frac{e\psi(0)}{2k_B T}\right) - exp\left(\frac{-e\psi(0)}{2k_B T}\right)\right] \quad (5)$$

where c is the ionic concentration, N is Avogadro's number, ε_r is the dielectric constant, ε_0 is the vacuum permittivity, and e is the electronic charge. If it is assumed that the surface is the plane of zero-shear, $\psi(0)$ is the ζ-potential. Inserting the charge per lipid obtained from the NR simulations, +0.032 e, into Eq (5), setting ε_r = 78.3 (the dielectric constant for bulk water at 298), and 64.7 Å^2 for the area/lipid[7] yields ζ = 11 mV. This value is well outside of the experimental value of 0, which has an uncertainty of approximately ±3 mV. In contrast, the charge per lipid obtained in the CW simulations, +0.0078 e, yields 2.7 mV for the same parameters, in much better agreement with experiment. Other values[38] for the effective dielectric at the bilayer surface are not considered for this estimate, because ε_r = 78.3 is used for scaling the mobility to a ζ-potential (Eq 1).

Recent work has indicated that vesicles of (neutral) POPC carry a slight overall negative charge,[39] but a previous study with stearoyloleoyl phosphatidylcholine (SOPC) indicated that unsaturated lipids have a residual negative charge due to impurities,[40] which would not ordinarily be present in a simulation. Simulations on other bilayers composed of neutral lipids may be helpful for future refinements of these parameters, and extensions to other ions.

The refined LJ parameters (the CW set) were validated by comparison of simulated and experimental deuterium order parameters for POPS and DMPG bilayers. It is clear from Figs. 8 and 9 that the agreement with these experimental measurements is considerably improved by the larger area/lipid value brought about by the use of the new NBFIX terms for sodium ion interactions (Table 5). For DMPG, the experimental trend in $|S_{CD}|$ observed for 0 and 0.1 M added NaCl is matched well in the simulations, and lends further support to the validity of the added terms. Again, this is consistent with the change in area/lipid observed in the DMPG simulations, in that the decrease in area at 0.1 M NaCl indicated in Table 3 leads to a slight increase in the order parameters. Experimental $|S_{CD}|$ contain a small contribution from collective motions not present in simulations of small patches of membrane, so a small overestimate in the magnitude of experimental order parameters is preferable to an underestimate.

The qualitative reduction of sodium binding to POPS effected by the changes in parameter set from BR to CW is illustrated in Fig 10. Fig. 11 compares the sodium ion distributions with respect to the carboxyl (top) and phosphate (bottom) groups of POPS for both sets. The distributions for CW are noticeably reduced in height in the lipid head group region, especially near the carboxylates (ca. −24 Å), and extend further into solution (−28 to −40 Å). The phosphate peak in CW is shifted toward the center of the bilayer, as expected from the increased surface area. In effect, the increased $R^{ij}_{\min}$ for sodium-lipid interactions in CW reduces ion binding. The lower binding leads to poorer shielding of surface electrostatics, increased repulsion among head groups, and increased surface area consistent with the drop

in $|S_{CD}|$ discussed above. Table 6 presents lifetime data for sodium binding to the carboxylate, phosphate and ester groups for the BR and CW simulations of POPS and DMPG. Both the average and maximum lifetimes are significantly longer for BR than CW, as anticipated from the change to the lipid/ion interaction potential.

Fig. 12 lends some insight as to why it is difficult to interpret the charge from simulations to an effective charge from electrophoresis experiments. The top panel plots the integrated charge/lipid of *only* lipid atoms as a function of distance from the bilayer center. As expected for all three sets, the charge is zero at the center, and monotonically decreases to −1 e by 30 Å, which is above the carboxyl group of the serine (see Fig 10). When Na^+ and Cl^- are included in the net charge (middle panel), there is a minimum at 26.5 Å (just past the serine peak), and values of −0.21 e for CW, indicating much weaker binding of Na+ than the other sets. Finally, the bottom panel of Fig 12 shows how the oriented water near the surface modulates the integrated charge. The profile is bimodal, and as many as three planes in the bilayer/water interface have the same charge.

Over-binding could occur with any ion, in principle, but ions with very strong interactions are more difficult to model accurately. Those are ions with a smaller radius like sodium or lithium, or divalent ions like calcium and magnesium. Problems due to over-binding to various molecular moieties can arise, even in the case of FF that was carefully parameterized to yield accurate models of ions at infinite dilution in bulk water. A complete inventory of all possible cases remains to be considered in detail in most biomolecular FF.

The good agreement with experiment for both small molecules and POPC, POPS, and DMPG bilayers presented here indicate that the lipid parameters do not require immediate adjustment. By implication, lipids with PS and PG head groups and different tails are adequately parameterized for simulations in sodium chloride. Extensions to other charged lipids are straightforward, but they should be validated. Likewise, the NBFIX values obtained here could be applied to other biopolymers, but also require validation. The environment on a membrane surface differs from that of a protein or DNA.

Acknowledgments

We thank Stuart McLaughlin and Wonpil Im for helpful discussions. The osmotic pressure and effective charge calculations were carried out on the IBM Blue Gene/P cluster Intrepid of the Argonne Leadership Computing Facility (ALCF). Dr. Luo's research was supported by the Early Science Postdoctoral Fellowship for Blue Gene/Q of ALCF. This research was also supported in part by the Intramural Research Program of the NIH, National Heart, Lung and Blood Institute, and utilized the high-performance computational capabilities at the National Institutes of Health, Bethesda, MD (NHLBI LoBoS cluster).

References

1. Brooks BR, Brooks CL, Mackerell AD, Nilsson L, Petrella RJ, Roux B, Won Y, Archontis G, Bartels C, Boresch S, Caflisch A, Caves L, Cui Q, Dinner AR, Feig M, Fischer S, Gao J, Hodoscek M, Im W, Kuczera K, Lazaridis T, Ma J, Ovchinnikov V, Paci E, Pastor RW, Post CB, Pu JZ, Schaefer M, Tidor B, Venable RM, Woodcock HL, Wu X, Yang W, York DM, Karplus M. Journal of Computational Chemistry. 2009; 30:1545–1614. [PubMed: 19444816]
2. Case DA, Cheatham T, Darden T, Gohlke H, Luo R, Merz KM Jr, Onufriev A, Simmerling C, Wang B, Woods R. J Comp Chem. 2005; 26:1668–1688. [PubMed: 16200636]
3. Bowers KJ, Chow E, Xu H, Dror RO, Eastwood MP, Gregersen BA, Klepeis JL, Kolossvary I, Moraes MA, Sacerdoti FD, Salmon JK, Shan Y, Shaw DE. Proceedings of the ACM/IEEE Conference on Supercomputing (SC06). 2006
4. Berendsen HJC, van der Spoel D, van Drunen R. Comp Phys Commun. 1995; 91:43–56.
5. Plimpton S. J Comp Phys. 1995; 117:1–19.

6. Phillips JC, Braun R, Wang W, Gumbart J, Tajkhorshid E, Villa E, Chipot C, Skeel RD, Kale L, Schulten K. Journal of Computational Chemistry. 2005; 26:1781–1802. [PubMed: 16222654]
7. Klauda JB, Venable RM, Freites JA, O'Connor JW, Tobias DJ, Mondragon-Ramirez C, Vorobyov I, MacKerell AD Jr, Pastor RW. Journal of Physical Chemistry B. 2010; 114:7830–7843.
8. Pastor RW, MacKerell AD Jr. J Phys Chem Letters. 2011; 2:1526–1532.
9. Berkowitz ML, Bostick DL, Pandit S. Chemical Reviews. 2006; 106:1527–1539. [PubMed: 16608190]
10. Jurkiewicz P, Cwiklik L, Vojtiskova A, Jungwirth P, Hof M. Biochimica Et Biophysica Acta-Biomembranes. 1818:609–616.
11. Berneche S, Roux B. Nature. 2001; 414:73–77. [PubMed: 11689945]
12. Roux B, Berneche S. Biophysical Journal. 2002; 82:1681–1684. [PubMed: 11898796]
13. Luo Y, Roux B. Physical Chemistry Letters. 2010; 1:183–189.
14. Verwey, EJW.; Overbeek, JTG. Theory of the Stability of Lyophobic Colloids. Courier Dover Publications; New York: 1948. reprint ed
15. McLaughlin S. Annual Review of Biophysics and Biophysical Chemistry. 1989; 18:113–136.
16. Pratt LR. J Phys Chem. 1992; 96:25–33.
17. Vorobyov I, Bekker B, Allen TW. Biophysical Journal. 2010; 98:2904–2913. [PubMed: 20550903]
18. Harder E, Roux B. Journal of Chemical Physics. 2008; 129
19. Winiski AP, McLaughlin AC, McDaniel RV, Eisenberg M, McLaughlin S. Biochemistry. 1986; 25:8206–8214. [PubMed: 3814579]
20. Petrache HI, Tu K, Nagle JF. Biophys J. 1999; 76:2479–2487. [PubMed: 10233065]
21. Petrache HI, Dodd SW, Brown MF. Biophys J. 2000; 79:3172–3192. [PubMed: 11106622]
22. Feller SE, Venable RM, Pastor RW. Langmuir. 1997; 13:6555–6561.
23. Klauda JB, Venable RM, MacKerell AD, Pastor RW. Computational Modeling of Membrane Bilayers. 2008; 60:1–48.
24. Petrache HI, Tristram-Nagle S, Gawrisch K, Harries D, Parsegian VA, Nagle JF. Biophys J. 2004; 86:1575–1586.
25. Mukhopadhyay P, Monticelli M, Tieleman DP. Biophys J. 2004; 86:1601–1609. [PubMed: 14990486]
26. Marra J. Biophys J. 1986; 50:815–825. [PubMed: 3790687]
27. Loew C, Riske KA, Lamy MT, Seelig J. Langmuir : the ACS journal of surfaces and colloids. 2011; 27:10041–9. [PubMed: 21732628]
28. Jorgensen WL, Chandrasekhar J, Madura JD, Impey RW, Klein ML. J Chem Phys. 1983; 79:926–935.
29. Durell SR, Brooks BR, Bennaim A. J Phys Chem. 1994; 98:2198–2202.
30. Beglov D, Roux B. J Chem Phys. 1994; 100:9050–9063.
31. Noskov SY, Roux B. Journal of Molecular Biology. 2008; 377:804–18. [PubMed: 18280500]
32. Durand-Vidal, S.; Simonin, J-P.; Turq, P. Electrolytes at Interfaces. Vol. 1. Kluwer Academic Publishers; Dordrecht, the Netherlands: 2000.
33. Zhang YH, Feller SE, Brooks BR, Pastor RW. J Chem Phys. 1995; 103:10252–10266.
34. Darden T, York D, Pedersen L. J Chem Phys. 1993; 98:10089–10092.
35. Klauda JB, Wu XW, Pastor RW, Brooks BR. J Phys Chem B. 2007; 111:4393–4400. [PubMed: 17425357]
36. Huster D, Arnold K, Gawrisch K. Biochemistry. 1998; 37:17299–17308. [PubMed: 9860844]
37. Seelig A, Seelig J. Biochemistry. 1974; 13:4839–4845. [PubMed: 4371820]
38. Kimura Y, Ikegami A. Journal of Membrane Biology. 1985; 85:225–231. [PubMed: 3839852]
39. Klasczyk B, Knecht V, Lipowsky R, Dimova R. Langmuir. 2010; 26:18951–18958. [PubMed: 21114263]
40. Pincet F, Cribier S, Perez E. Eur Phys J B. 1999; 11:127–130.

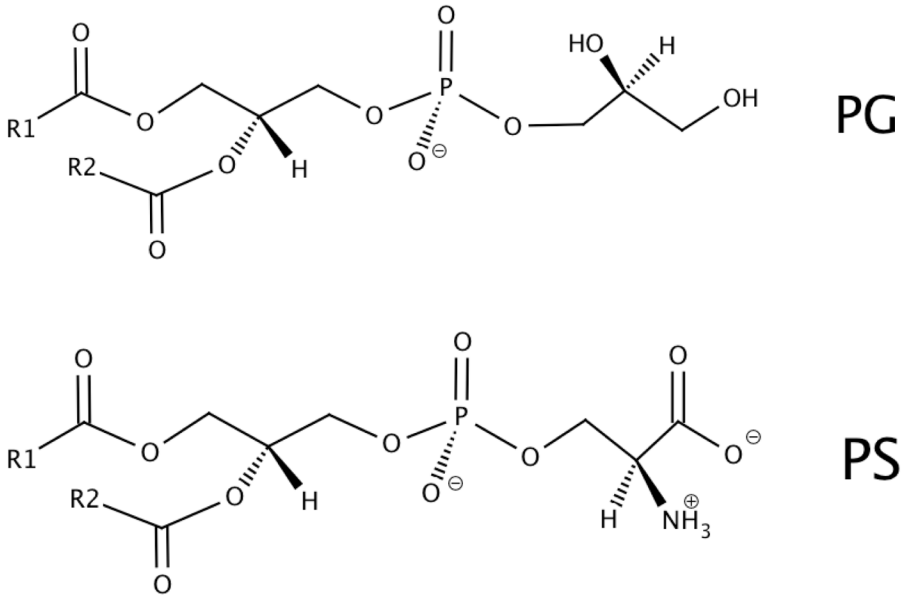

Figure 1.
Molecular structures of anionic lipid headgroups phosphatidylglycerol (PG) phosphatidylserine (PS). For DMPG, both R1 and R2 are myristate chains; for POPS, the R1 chain is palmitate, and the R2 chain is oleate.

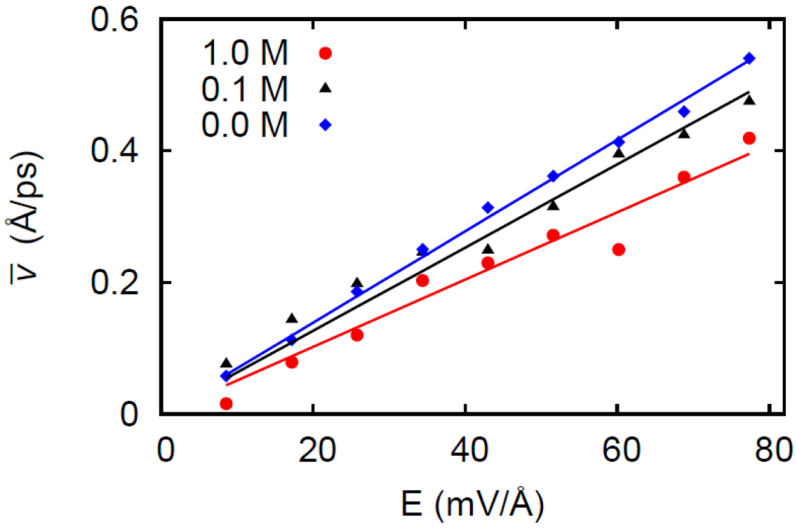

Figure 2.
The average drift velocity v as a function of electric field applied to 3 different concentrations NaCl solution with a single NaOAc molecule.

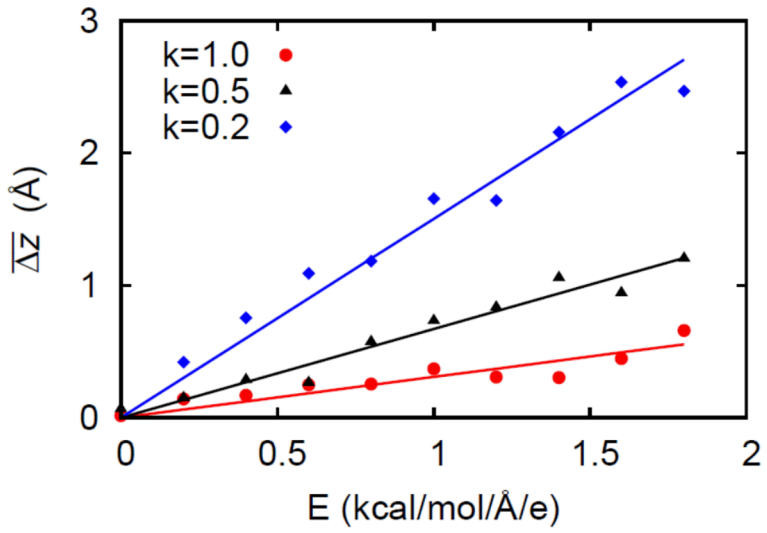

Figure 3.
The average z-displacement of acetate ion in 0.1 M NaCl under 3 different harmonic restraints vs electric field.

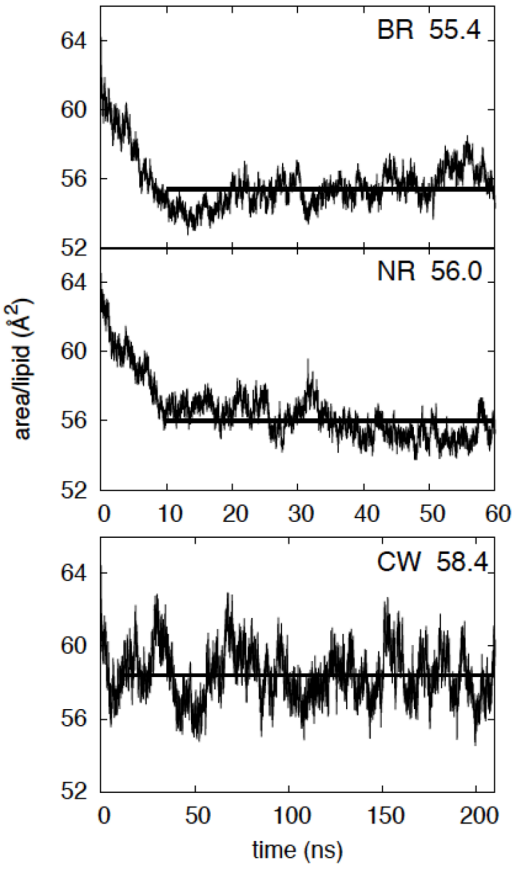

Figure 4.
Area/lipid time series and average area (heavy flat line) for POPS simulations with 0.1 M excess NaCl; the NBFIX terms are only included in the CW simulation.

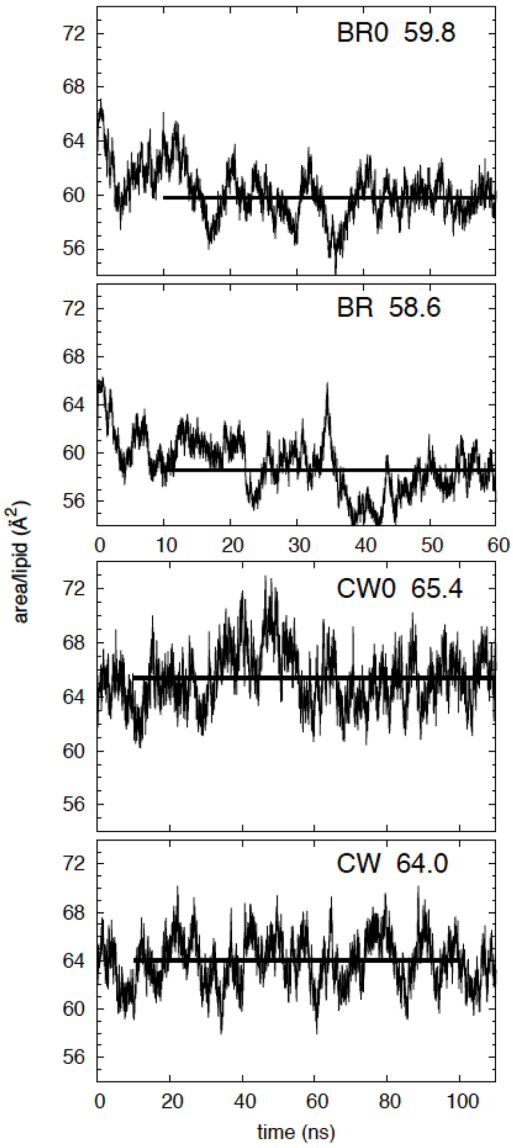

Figure 5.
Area/lipid time series and average area (heavy flat line) for DMPG simulations; BR0 and CW0 have no excess NaCl, while BR and CW have 0.1 M excess NaCl. The CW simulations include the NBFIX terms.

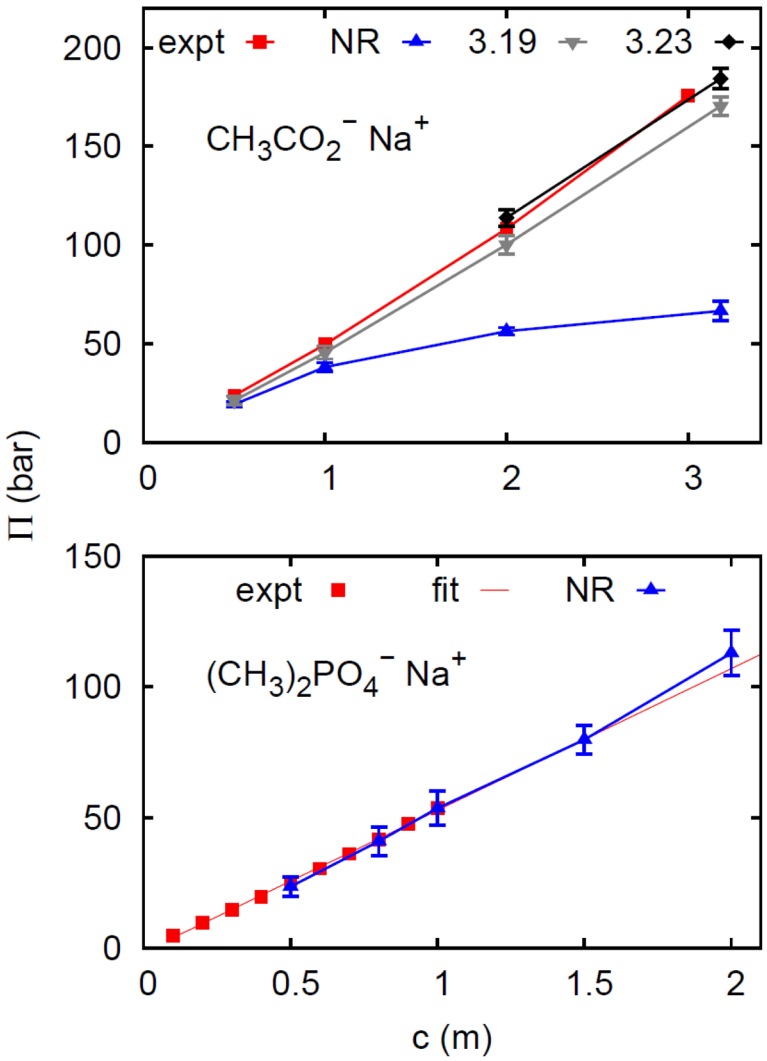

Figure 6.

Osmotic pressure (Π) as a function of molal concentration for acetate (upper) and dimethylphosphate (lower) sodium salts. The fit to experiment line is extrapolated for comparison to simulation at higher *c* values. Error bars are from replicate 2 ns simulations.

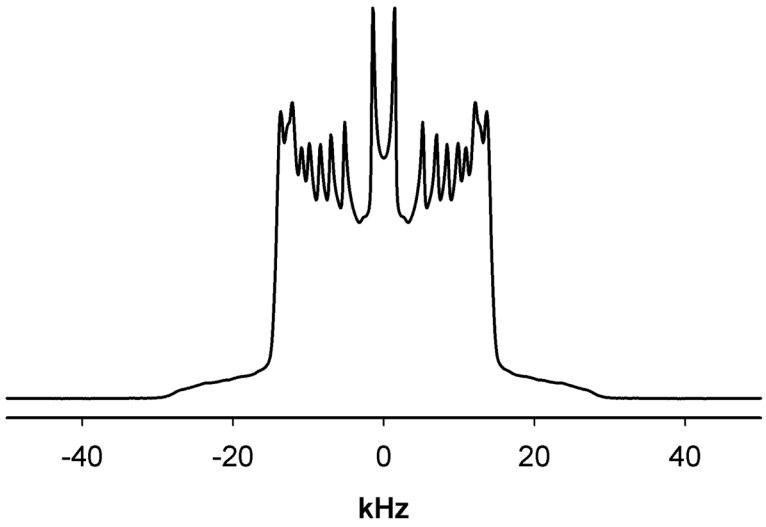

Figure 7.
Deuterium NMR spectrum for POPC-d31 in excess 0.1 M NaCl.

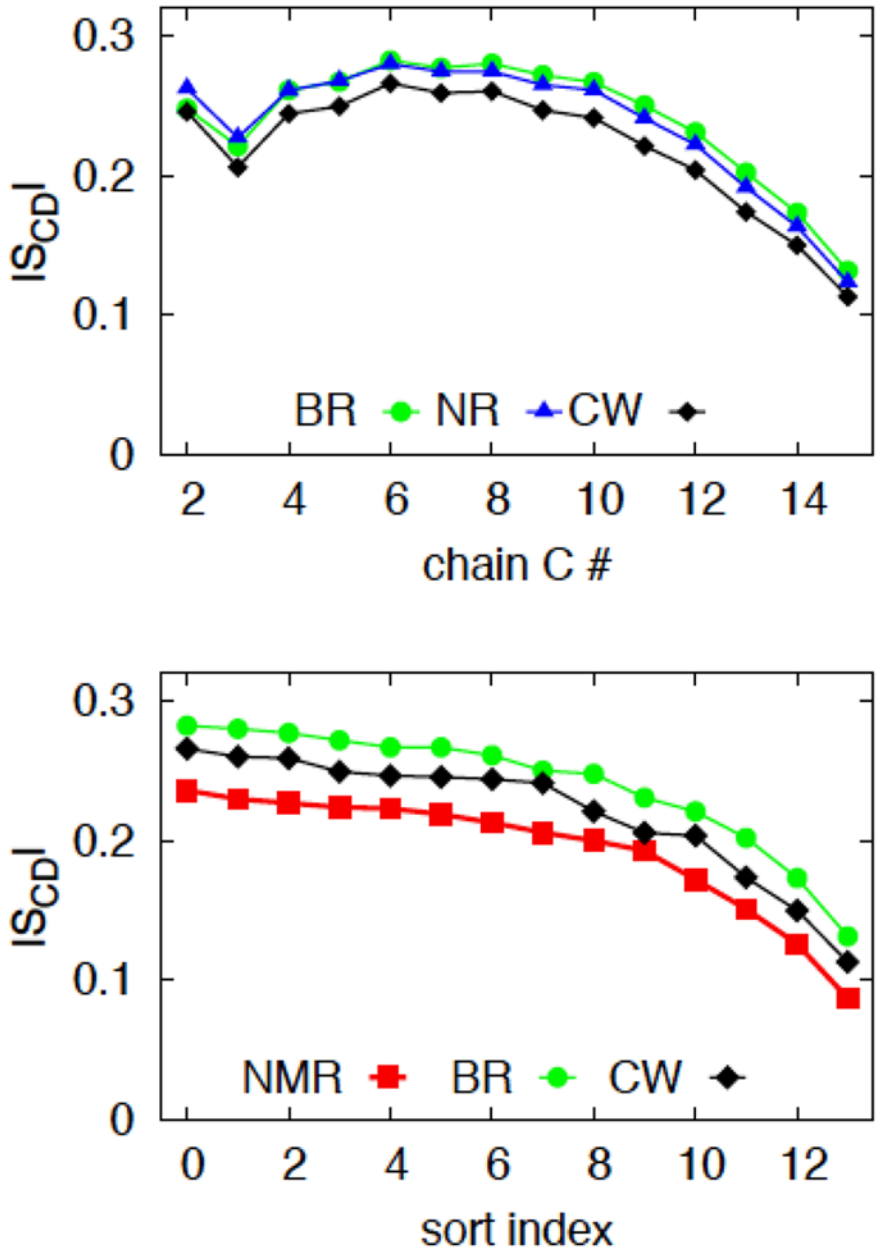

Figure 8.
POPS simulation order parameters as a function of palmitate chain position, top; experimental order parameters compared to simulation data sorted by decreasing S_{CD} value, bottom.

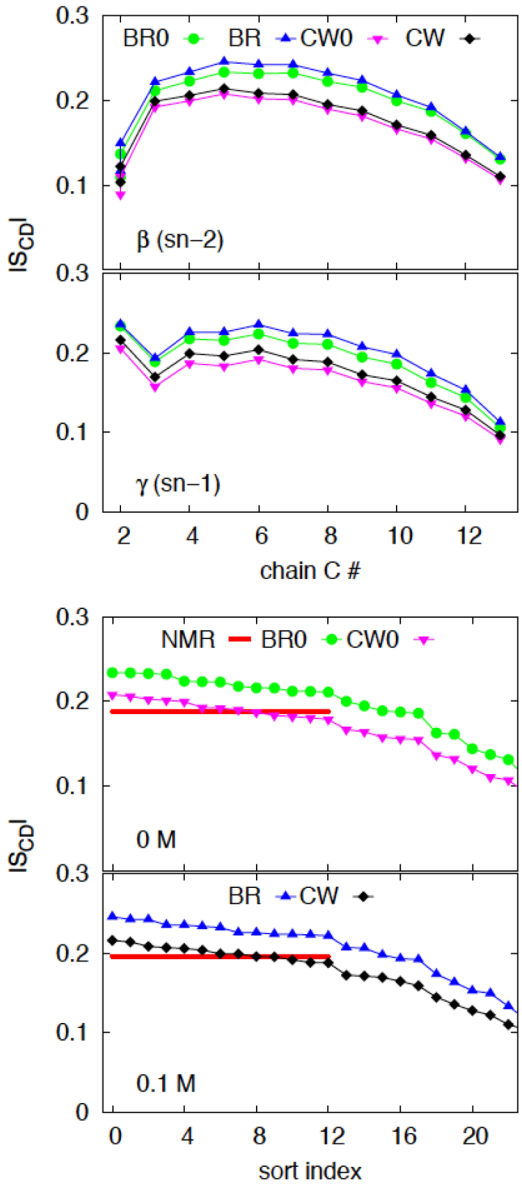

Figure 9.
DMPG lipid chain order parameters from the simulations plotted by chain position for each chain, top 2 panels; sorted order parameters for both chains compared to NMR values at 0 and 0.1 M NaCl, bottom 2 panels.

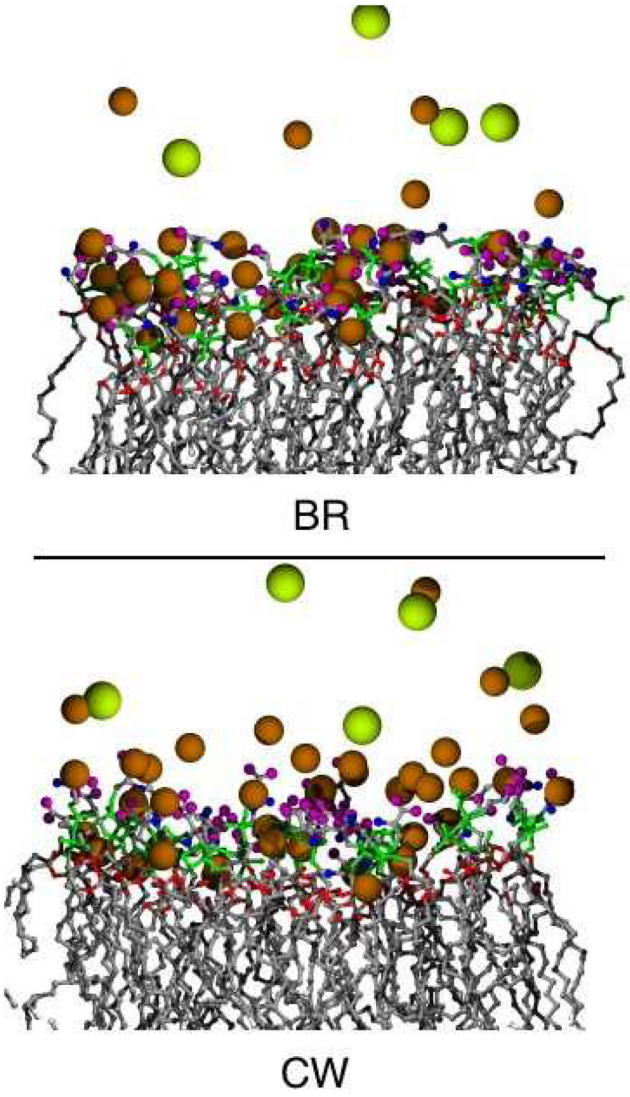

Figure 10.
Representative snapshots from simulations of POPS at 0.1 M NaCl with the BR (top) and CW (bottom) ion/lipid parameters. Sodium and chloride are brown and green spheres, respectively. Lipid atoms in stick form with carbon grey, ester oxygens red, phosphate green, nitrogen blue, and carboxylate oxygens magenta. Waters are omitted for clarity.

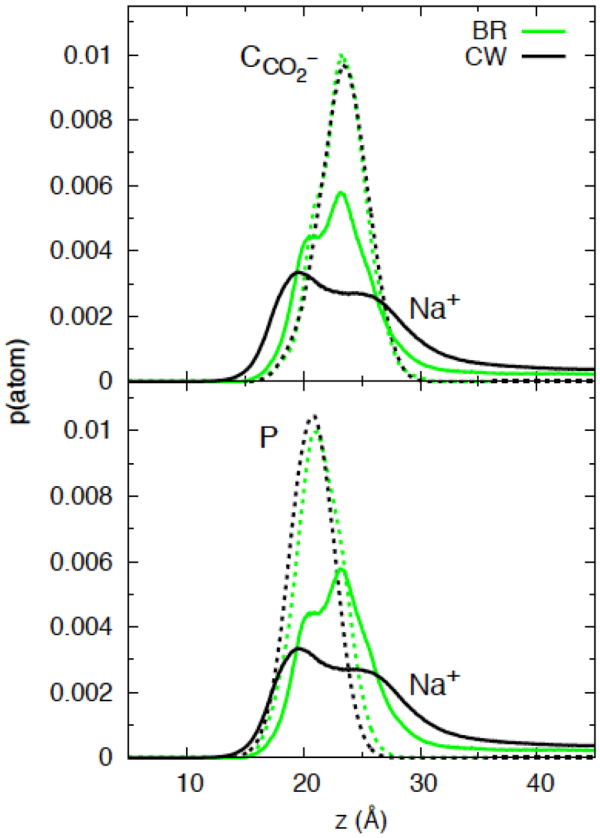

Figure 11.
Simulation z distributions for sodium ions (solid lines) in POPS bilayers vs the carboxylate carbon (dashed, top) and phosphate P (dashed, bottom). Distributions are time averaged and symmetrized; the bilayer cleavage plane is at z=0.

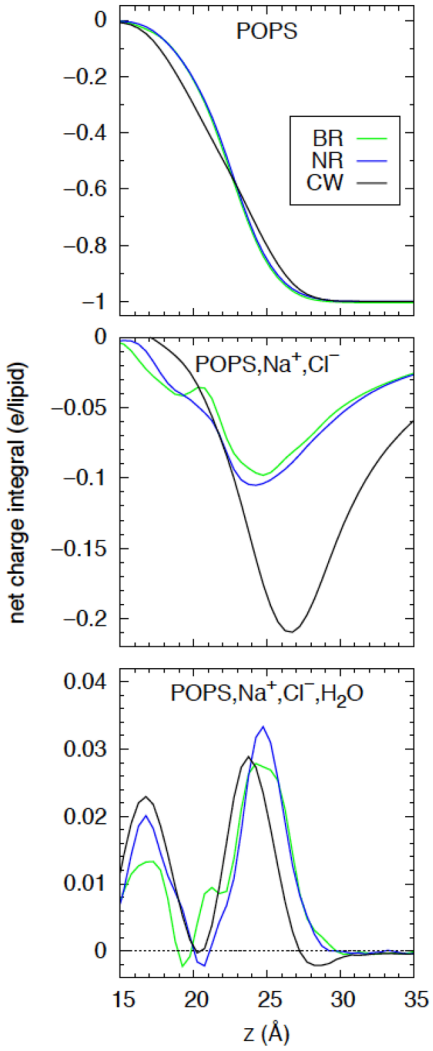

Figure 12.
Net integrated charge for assorted components of POPS bilayer in 0.1 M NaCl: only lipid atoms (top); lipid plus salt (middle); lipid, salt, and water (bottom).

TABLE 1

Three model systems and the calculated electrophoretic mobility.

Salt conc.	Acetate	Na^+	Cl^-	Water	Mobility ($Å^2 \cdot ps^{-1}\ mV^{-1}$)
0 M	1	0	0	3444	0.0069
0.1 M	1	6	5	3444	0.0063
1 M	1	67	66	3706	0.0051

TABLE 2

The calculated effective charge Q_{eff} (in e) of an acetate ion in 1 M NaCl aq. solution from three different methods.

Method	Q_{eff}
Drift velocity (Eq 3)	−0.74
Einstein-Smoluchowski (Eq 4)	−0.62
Harmonic restraint (Eq 2)	−0.63

TABLE 3

Excess NaCl concentrations, area/lipid, and designations based on the ion treatment (parameters) and concentration for the POPS and DMPG validation simulations; standard errors for the area/lipid are given in parentheses.

Lipid	Excess NaCl, M	Run Time (ns)	<area/lipid>, Å^2	Designation[a]
POPS	0.1	60	55.4 (0.1)	BR
“	0.1	60	56.0 (0.1)	NR
“	0.1	210	58.4 (0.1)	CW
DMPG	0	60	59.8 (0.3)	BR0
“	0.1	60	58.5 (0.4)	BR
“	0	110	65.4 (0.3)	CW0
“	0.1	110	64.0 (0.2)	CW

[a]Details of designation abbreviations are given in the Methods section.

TABLE 4

Lennard-Jones well-depths ε (kcal/mol) and radii ½ R_{min} (Å) for relevant atoms

Atom	Atom type	ε	½ R_{min}
Na^+ [a]	SOD	−0.0469	1.36375
Na^+ [b]	SOD	−0.0469	1.4107
Cl^-	CLA	−0.150	2.27
O on acetate anion	OCL	−0.12	1.70
=O on phosphate	O2L	−0.12	1.70
=O on acetate ester	OBL	−0.12	1.70

[a] From Beglov and Roux,[30] distributed with C36 lipids.

[b] From Noskov and Roux.[31]

TABLE 5

Comparison of Lennard-Jones parameter R^{ij}_{min} (Å) for relevant pairs from arithmetic combining rule (unmodified) and as modified by NBFIX for the current work. E_{min} (kcal/mol) is the same for both sets.

		R^{ij}_{min}	
Ion pair	**E_{min}**	**unmodified**	**NBFIX**
SOD-CLA [a]	−0.08388	3.6807	3.731
SOD-OCL [b]	−0.07502	3.1107	3.23
SOD-O2L [c]	−0.07502	3.1107	3.16
SOD-OBL [c]	−0.07502	3.1107	3.13

[a] From Luo and Roux.[13]

[b] From this work, osmotic pressure calculation of NaOAc solution.

[c] From this work, effective charge calculation of POPC lipid bilayer in NaCl solution.

TABLE 6

Sodium ion binding lifetime data for lipid O atoms with large partial charges from simulations with 0.1 M excess NaCl.

System, Designation	Moeity	<lifetime>, ps	Maximum Lifetime, ns
POPS, BR	carboxylate	163.9	> 20
	phosphate	163.9	> 20
	ester	70.8	7.5
POPS, CW	carboxylate	20.3	7.7
	phosphate	51.9	17.0
	ester	67.0	7.5
DMPG, BR	phosphate	113.2	> 10
	ester	82.2	8.6
DMPG, CW	phosphate	39.0	3.3
	ester	61.6	2.2